Journal of the American Heart Association

ORIGINAL RESEARCH

Serial Assessment of Right Ventricular Deformation in Patients With Hypoplastic Left Heart Syndrome: A Cardiovascular Magnetic Resonance Feature Tracking Study

Luca Mitch Kanngiesser; Sandra Freitag-Wolf, PhD; Simona Boroni Grazioli; Dominik Daniel Gabbert, PhD; Jan Hinnerk Hansen, MD; Anselm Sebastian Uebing, MD; Inga Voges, MD

BACKGROUND: As right ventricular dysfunction is a major cause of adverse outcome in patients with hypoplastic left heart syndrome, the aim was to assess right ventricular function and deformation after Fontan completion by performing 2-dimensional cardiovascular magnetic resonance feature tracking in serial cardiovascular magnetic resonance studies.

METHODS AND RESULTS: Cardiovascular magnetic resonance examinations of 108 patients with hypoplastic left heart syndrome (female: 31) were analyzed. Short-axis cine images were used for right ventricular volumetry. Two-dimensional cardiovascular magnetic resonance feature tracking was performed using long-axis and short-axis cine images to measure myocardial global longitudinal, circumferential, and radial strain. All patients had at least 2 cardiovascular magnetic resonance examinations after Fontan completion and 41 patients had 3 examinations. Global strain values and right ventricular ejection fraction decreased from the first to the third examination with a significant decline in global longitudinal strain from the first examination to the second examination (median, first, and third quartile: –18.8%, [–20.5;–16.5] versus –16.9%, [–19.3;–14.7]) and from the first to the third examination in 41 patients (–18.6%, [–20.9;–15.7] versus –15.8%, [–18.7;–12.6]; *P*-values <0.004). Right ventricular ejection fraction decreased significantly from the first to the third examination (55.4%, [49.8;59.3] versus 50.2%, [45.0;55.9]; *P*<0.002) and from the second to the third examination (53.8%, [47.2;58.7] versus 50.2%, [45.0;55.9]; *P*<0.0002).

CONCLUSIONS: Serial assessment of cardiovascular magnetic resonance studies in patients with hypoplastic left heart syndrome after Fontan completion demonstrates a significant reduction in global strain values and right ventricular ejection fraction at follow-up. The significant reduction in global longitudinal strain between the first 2 examinations with non-significant changes in right ventricular ejection fraction suggest that global longitudinal strain measured by 2-dimensional cardiovascular magnetic resonance feature tracking might be a superior technique for the detection of changes in myocardial function.

Key Words: 2D cardiovascular magnetic resonance feature tracking ■ Fontan circulation ■ hypoplastic left heart syndrome ■ myocardial dysfunction ■ strain

Hypoplastic left heart syndrome (HLHS) is one of the most severe forms of congenital heart disease with fatal outcome if untreated.[1] It is characterized by hypoplasia of the left sided heart structures, including mitral and aortic valvular atresia or stenosis as well as hypoplasia of the ascending aorta.[2] The established surgical treatment strategy involves a 3-stage palliation with creation of a total cavopulmonary

Correspondence to: Inga Voges, MD, Department of Congenital Heart Disease and Pediatric Cardiology, Arnold-Heller-Str. 3, Haus 9, University Hospital Schleswig-Holstein, Campus Kiel. Email: inga.voges@uksh.de

Supplemental Material for this article is available at https://www.ahajournals.org/doi/suppl/10.1161/JAHA.122.025332

For Sources of Funding and Disclosures, see page 9.

JAHA is available at: www.ahajournals.org/journal/jaha

CLINICAL PERSPECTIVE

What Is New?

- Most hypoplastic left heart syndrome studies have assessed right ventricle (RV) function and size during staged palliation but serial data about RV deformation after Fontan completion are rare.
- There is evidence that myocardial longitudinal strain and strain rate decrease during Fontan follow-up before a decline in RV ejection fraction manifests.
- Combined volumetry and analysis of long-axis function using cardiovascular magnetic resonance feature tracking seem to be suitable to detect RV dysfunction early, but further research is warranted to develop protocols and functional analysis tools best suited to assess the abnormally loaded RV in hypoplastic left heart syndrome.

What Are the Clinical Implications?

- Regular and life-long follow-up of patients with hypoplastic left heart syndrome in specialized congenital heart centers including monitoring of RV size and function is mandatory.
- Current practice aims for a repeated cardiovascular magnetic resonance scan every 3 to 5 years depending on the patient's condition and future serial studies may be supplemented by additional cardiac markers, such as cardiac laboratory markers.
- The findings of this study encourage to proceed with further research to detect reliable factors that contribute to early myocardial RV dysfunction in patients with hypoplastic left heart syndrome.

Nonstandard Abbreviations and Acronyms

2D-CMR-FT	2-dimensional cardiovascular magnetic resonance feature tracking
BSA	body surface area
GCS	global circumferential strain
GLS	global longitudinal strain
GRS	global radial strain
HLHS	hypoplastic left heart syndrome
Neo-AVR	neo-aortic valve regurgitation
RVEDVi	right ventricular end-diastolic volume index
RVEF	right ventricular ejection fraction
RVESVi	right ventricular end-systolic volume index
RVMMi	right ventricular myocardial mass index
RVSVi	right ventricular stroke volume index
TCPC	total cavopulmonary connection
TR	tricuspid valve regurgitation

connection (TCPC) being the third step.[3] Although survival rates for patients born in the 21st century compared with those born at the early 90s increased,[4,5] information about right ventricular (RV) function and deformation in patients with HLHS in Fontan circulation is still sparse.[6,7]

In a recent study, our group showed a significant increase in RV volumes with only mild reduction in RV ejection in patients with HLHS during serial follow-up.[8]

Several studies have demonstrated that echocardiography and two-dimensional speckle tracking echocardiography are suitable to evaluate RV function through staged palliation.[9–11]

2D-CMR-FT can be used in patients with HLHS.[7] It has been shown to be comparable to 2-dimensional speckle tracking echocardiography for the assessment of longitudinal strain, allows an exact measurement of ventricular size and ejection fraction (EF) and has the advantage of unlimited imaging windows.[12]

The aim of this study was to use 2D-CMR-FT to investigate global and regional right ventricular myocardial deformation in a large cohort of patients with HLHS during protocolized serial follow-up. Furthermore, we aimed to evaluate the value of deformation parameters to detect early RV dysfunction in patients with HLHS.

METHODS

The data that support the findings of this study are available from the corresponding author upon reasonable request within the limits of ethical and legal restrictions.

Ethical Statement

The study protocol conforms to the ethical guidelines of the 1975 Declaration of Helsinki and was approved by the local ethics committee (ID Nr.: D503/20, date of the approval: 10th August 2020). Informed consent was obtained from the parents or guardians of the children enrolled into the study.

Patients

One hundred and eight pediatric and adult patients with HLHS [median age at first scan 4.5 years (1st and 3rd quartile: 3.9;6.4 years)] who underwent clinical CMR imaging as part of routine clinical follow-up

between December 2005 and July 2021 were included. Inclusion criteria were: (1) a completed Fontan circulation, (2) the availability of at least 2 serial CMR studies after Fontan completion, and (3) no contraindications for CMR. Patients were excluded if: (1) Fontan circulation was not completed, (2) only one CMR study after Fontan completion was performed, and (3) if CMR data sets were of insufficient quality.

CMR studies with axial long-axis cine views and in most cases a complete stack of short-axis cines were required to measure RV deformation, volumes, and RVEF. Patients with insufficient data sets were excluded. Patient characteristics were obtained from medical records and included underlying diagnosis, variables related to surgical palliation and history of complications (protein-losing enteropathy, plastic bronchitis, arrhythmias, thromboembolic events). Data from the clinical follow-up included oxygen saturation and current medication.

CMR Acquisition

CMR was performed using a 3T or 1.5T scanner. In small children conscious sedation with midazolam and propofol in younger children was needed (154/257 CMR studies). In sedated patients, heart rate, respiratory motion, oxygen saturation and noninvasive blood pressure were monitored.

Short-axis cine stacks were acquired using gradient echo or steady-state free precession cine imaging with retrospective ECG gating, to measure RV volumes, myocardial mass, and function. The scan parameters were as follows: field of view 175 to 450 mm, slice thickness 5 to 8 mm, 20 to 30 cardiac phases, no slice gap, non-breath-hold in sedated children, breath-hold in awake patients. In addition, axial long-axis cine images showing the atria and right ventricle in a similar manner as a standard 4-chamber view was obtained with the following scan parameters: field of view 175 to 400 mm, slice thickness 5 to 8 mm, 20 to 30 cardiac phases, non-breath-hold in sedated children, breath-hold in awake patients.

CMR Analysis

Post-processing was performed using commercially available software (cvi42 for Cardiovascular MRI, Circle Cardiovascular Imaging, Calgary, Canada; Medis Suite Solutions, Medical Imaging Software, Leiden, the Netherlands). All CMR measurements were performed by the same observer (LK) and carefully checked by a senior observer specializing in congenital CMR (IV).

Assessment of RV end-diastolic and end-systolic volumes (RVEDV, RVESV), myocardial mass and RVEF was performed by manual tracing of endocardial contours for each slice from the stack of short-axis cine images at end-systole and end-diastole using Simpson's method.[13] The position of the tricuspid valve was confirmed by linking the short-axis stack to a long-axis view of the RV. Trabeculations and papillary muscles were included into the ventricular volume. All volumes and ventricular mass were indexed to body surface area (BSA).

Assessments of RV myocardial peak strain, strain rate, velocity and displacement were performed based on manual tracing of the endocardial and epicardial contours in ECG gated CMR images (QStrain, Medis Medical Imaging Systems BV). Peak strain and strain rate values were measured as these parameters are relatively load independent or less sensitive to expected ventricular dyssynchrony and temporal resolution.[11,14–17] Global circumferential (GCS) and radial strain (GRS) and strain rates (GCSR and GRSR) were measured from short-axis cine images at 3 ventricular levels (basal, mid-ventricular and apical); see Figure 1. Global longitudinal strain and strain rate values (GLS and GLSR; Figure 1) were analyzed from axial long-axis cine images showing the atria and right ventricle. Simultaneously, velocity and displacement were measured in longitudinal, radial, and circumferential direction. Arithmetic means of segmental values in long-axis images (7 segments) and short-axis images (16 segments) were calculated for the analysis of global deformation parameters.

The degree of tricuspid and neo-aortic valve regurgitation (TR, neo-AVR) was documented from CMR and echocardiographic reports and was classified as none, trivial (regurgitant fraction <5%), mild (regurgitant fraction <20%), moderate (regurgitant <40%), and severe (regurgitant fraction 40% and higher).

In 9/257 CMR studies imaging data sets were incomplete or of reduced quality and did not allow short-axis deformation analysis. In 7 cases RV volumetry was performed from transaxial cine stacks.

To assess inter-observer variability, myocardial strain parameters (SBG, LK) and RV volumetry parameters (IV, LK) were measured twice by 2 experienced operators in 30 patients.

Statistical Analysis

Statistical analysis was performed using MedCalc version 19.3.1 (MedCalc Software Ltd, Belgium) and SPSS version 25. Normal distribution was assessed using the Shapiro-Wilk test and checked visually from histograms. Normally distributed continuous variables are presented as mean and standard deviation or as median with first and third quartile (Q1;Q3) in non-normally distributed data. Categorical variables are expressed as total counts with percentages. Paired samples Wilcoxon test was performed to compare results between serial CMR examinations. Correlations of RVEF and strain parameters were assessed using Spearman's coefficient of rank correlation for non-normally distributed data.

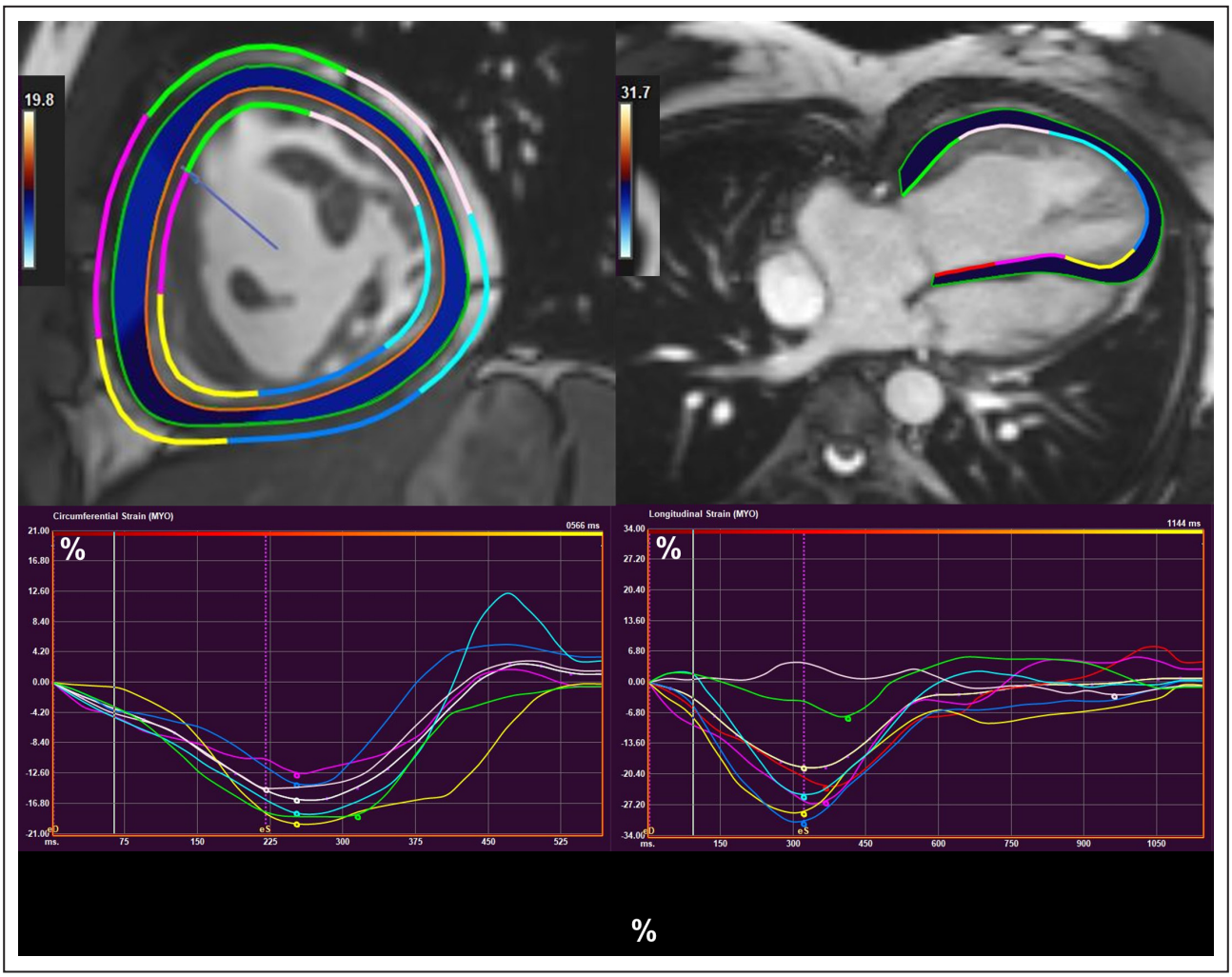

Figure 1. Segmental CMR feature tracking in the short- and long-axis of the RV.
CMR indicates cardiovascular magnetic resonance; and RV, right ventricle.

An explorative factor analysis based on a principal components method (Varimax) was performed to find the variables best suitable to detect serial RV changes in patients with HLHS.[18] The number of factors was determined by exploiting the decrease in the eigenvalues indicating the explained overall variance.

Inter-observer variability was assessed with the intraclass correlation coefficient (ICC). ICC values between 0.5 and 0.75 indicate moderate, values between 0.75 and 0.9 indicate good and values >0.9 indicate excellent reliability. Considering multiple testing the significance level was adjusted by Bonferroni correction to 0.006. The global significance level of 5% was divided by the number of comparisons at 3 time points which were additionally multiplied by 3 as considering the 3 main post-processing categories (volumetry and feature tracking parameters in short-axis and long-axis views, respectively). This calculation resulted in a corrected significance level of 0.006.

RESULTS

Patient Characteristics

Data could be obtained from 108 patients with HLHS. A short overview is shown in Table 1 and additional patient characteristics are displayed in Supplemental Material (Table S1).

The first scan was performed at a median age of 4.5 (3.9;6.4) years and 1.8 (1.3;3.2) years after TCPC completion. TCPC was completed at a median age of 2.5 (2.2;2.9) years. The median interval between the first and second examination was 5.2 (4.8;6.0) years and between the first and third scan 10 (8.8;11.7) years respectively.

Most patients had an intraatrial lateral tunnel (n=103, 95.4%; extracardiac conduit: n=5, 4.6%). Mild TR and trivial neo-AVR were common (third CMR examination: 63.4% and 48.8%, respectively; Tables 1 and S1).

Table 1. Patient Characteristics

Parameters	1st CMR (n=108)	2nd CMR (n=108)	3rd CMR (n=41)
Age, y	4.5 [3.9;6.4]	10.1 [9.1;12.5]	15.3 [14.0;17.2]
Female/male (n, %)	31/77 (28.7%/71.3%)	31/77 (28.7%/71.3%)	11/30 (26.8%/73.2%)
Weight, kg	17.0 [15.6;20.0]	31.0 [26.9;37.6]	54.0 [44.8;63.3]
Height, cm	104.5 [100.0;114.0]	137.0 [130.0;150.5]	163.0 [154.5;173.0]
BMI, kg/m²	15.7 [14.7;16.6]	16.2 [15.3;18.1]	19.5 [16.9;23.1]
Heart rate, bpm	83.0 [75.0;89.0]	80.0 [70.0;90.0]	78.1 [72.3;86.3]
DBP, mm Hg	45.0 [41.0;51.8]	56.0 [47.0;66.0]	67.0 [58.0;78.0]
SBP, mm Hg	85.0 [80.0;90.8]	100.0 [90.0;116.0]	117.0 [106.8;129.5]
Oxygen saturation (%)	90.0 [87.0;94.0]	91.0 [88.5;95.0]	92.0 [88.0;95.0]
Intraatrial lateral tunnel (n, %)	103 (95.4%)	103 (95.4%)	41 (100%)
Extracardiac conduit (n, %)	5 (4.6%)	5 (4.6%)	0 (0%)
Open Fenestration (n, %)	79 (73.1%)	70 (64.8%)	22 (53.7%)

Data are presented as frequencies (%) or median [first and third quartile]. BMI indicates body mass index; bpm, beats per minute; CMR indicates cardiovascular magnetic resonance; DBP, diastolic blood pressure; SBP, systolic blood pressure; and y, years.

CMR Results

There was a significant decrease in GLS and myocardial GLSR from the first to the second and the third examination (all *P*-values <0.004, Table 2 and Figure 2A). GCSR decreased significantly from the first to the third scan (*P*=0.0039, Table 2). GCS, GRS, and GRSR did not change significantly between examinations. RVEF decreased significantly from the first to the third and from the second to the third examination (*P*-values <0.002, Table 3 and Figure 2B); the slight decrease in RVEF between the first and second scan did not reach statistical significance.

Indexed RV end-diastolic and end-systolic volumes increased significantly from the first examination to the second and to the third examination (Table 3). Median right ventricular myocardial mass index (RVMMi) increased significantly between the first and second scan but not significantly between the first and third examination. GCS and GLS correlated negatively with RVEF (GCS: Spearman's r=−0.57 to −0.69; GLS: −0.32 to −0.61; all *P*-values <0.0008; Figure 3).

There were no significant changes for the motion parameters (displacement and velocity) across the 3 examinations (Table 2).

Table 2. Results From CMR Feature Tracking

Parameters	1st CMR (n=108)	2nd CMR (n=108)	3rd CMR (n=41)
GLS (%)	−18.8 [−20.5;−16.5]	−16.9 [−19.3;−14.7]	−15.8 [−18.7;−12.6]
GCS (%)	−23.0 [−25.4;−19.7]	−22.1 [−24.8;−19.3]	−21.3 [−24.7;−18.5]
GLSR (1/s)	−1.2 [−1.4;−1.0]	−1.0 [−1.2;−0.9]	−0.9 [−1.1;−0.8]
GCSR (1/s)	−1.3 [−1.5;−1.1]	−1.2 [−1.4;−1.0]	−1.1 [−1.3;−1.0]
GRS (%)	58.5 [47.9;72.9]	57.1 [45.0;71.2]	53.8 [42.3;68.2]
GRSR (1/s)	2.7 [2.3;3.1]	2.6 [2.2;3.2]	2.4 [2.0;2.5]
Longitudinal velocity, cm/s	1.7 [1.4;2.1]	1.8 [1.6;2.3]	2.0 [1.7;2.5]
Longitudinal displacement, mm	1.6 [1.1;2.2]	1.9 [1.3;2.4]	1.8 [1.3;2.9]
Rotation velocity, deg/s	37.2 [31.5;45.6]	33.9 [28.5;41.6]	30.2 [24.5;39.0]
Rotation displacement, deg	3.7 [2.4;5.6]	4.3 [2.8;5.7]	4.0 [2.4;5.6]
Radial velocity, cm/s	2.5 [2.2;2.9]	2.7 [2.4;3.1]	2.8 [2.5;3.3]
Radial displacement, mm	5.3 [4.9;6.0]	5.8 [5.1;6.3]	6.2 [5.0;6.8]

Parameters are myocardial arithmetic means; Data are presented as median [first and third quartile]. CMR indicates cardiovascular magnetic resonance; GCS, global circumferential strain; GCSR, global circumferential strain rate; GLS, global longitudinal strain; GLSR, global longitudinal strain rate; GRS, global radial strain; and GRSR, global radial strain rate.

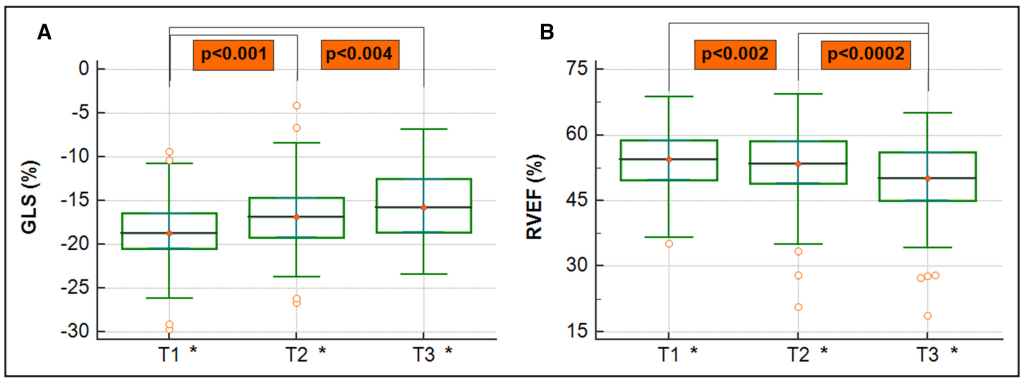

Figure 2. A and B, Box and whisker plots illustrating results for myocardial GLS (A) and RVEF (B) across the 3 CMR scans.

*n=108 at first first and second scan, n=41 at third scan; time points (T). CMR indicates cardiovascular magnetic resonance; GLS, global longitudinal strain; and RVEF, right ventricular ejection fraction.

Factor Analysis

Factor analysis was performed to find the CMR parameters best suited to detect serial RV changes in HLHS patients. For this analysis, 99 pairs of complete first and second CMR studies were used.

With 3 factors 54% of the overall variance could be explained. The first domain contained RVEF, and feature tracking parameters derived from the short axis. The second domain included RV volumes and the third domain comprised feature tracking parameters from long-axis views. Results are shown in Supplemental Material (Table S2).

Reproducibility of RV Measurements

Good to excellent inter-observer agreement was shown for right ventricular volumetric parameters. The intraclass correlation coefficient ranged from 0.90 to 0.99.

Moderate to excellent inter- and intra-observer agreement was found for myocardial strain parameters. ICC coefficients for inter-observer agreement were 0.34 in GRS, 0.79 in GCS and 0.84 in GLS. Intra-observer agreement ranged from 0.66 in GRS to 0.90 in GLS and 0.91 in GCS, respectively.

DISCUSSION

This is the largest single center CMR study that assessed serial changes in RV deformation and function in patients with HLHS after Fontan completion. The results demonstrate that myocardial GLS and GLSR decrease earlier than RVEF suggesting that CMR feature tracking might be superior to volume based functional parameters such as RVEF in detecting RV dysfunction early.

Factor analysis demonstrated that serial RV changes over time can be best described by a combination of CMR volumetry and 2D-CMR-FT parameters.

Table 3. Results From CMR volumetry

Parameters	1st CMR (n=108)	2nd CMR (n=108)	3rd CMR (n=41)
RVEDV, mL	65.8 [53.9;79.8]	104.1 [89.4;132.1]	171.6 [145.6;198.8]
RVESV, mL	29.8 [22.7;37.8]	49.4 [39.4;64.0]	83.0 [63.8;105.7]
RVSV, mL	33.8 [30.3;40.9]	54.4 [47.3;66.9]	80.7 [73.1;92.9]
RVEF, %	54.4 [49.7;58.7]	53.4 [48.9;58.6]	50.2 [45.0;55.9]
RVEDVi, mL/m²	88.3 [74.1;104.9]	95.9 [82.8;113.5]	107.9 [94.2;132.5]
RVESVi, mL/m²	40.8 [30.2;50.7]	44.0 [34.8;57.3]	52.0 [43.5;71.1]
RVSVi, mL/m²	47.7 [42.7;56.1]	52.7 [43.2;59.9]	53.3 [46.1;60.4]
RVMM, g	34.0 [28.3;40.4]	56.3 [43.9;73.3]	76.1 [63.0;94.4]
RVMMi, g/m²	47.3 [39.0;54.9]	50.3 [42.7;59.8]	49.6 [44.2;58.4]
Cardiac index, L/min per m²	4.1 [3.2;4.6]	4.0 [3.3;4.8]	4.2 [3.5;4.9]

Data are presented as median [first and third quartile]. CMR indicates cardiovascular magnetic resonance; EDV, end-diastolic volume; EF, ejection fraction; ESV, end-systolic volume; MM, myocardial mass; RV, right ventricle; RVEDVi, right ventricular end-diastolic volume index; RVEF, right ventricular ejection fraction; RVESVi, right ventricular end-systolic volume index; RVMMi, right ventricular myocardial mass index; RVSVi, right ventricular stroke volume index; and SV, stroke volume.

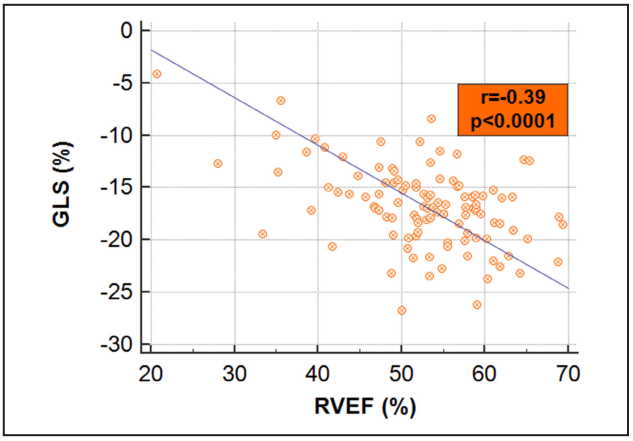

Figure 3. Spearman's rank correlation exemplarily for myocardial GLS and RVEF at second scan.
GLS indicates, global longitudinal strain; and RVEF, right ventricular ejection fraction.

Changes in RV Deformation and Motion, RV Function, and RVMMi

Only few studies have assessed longitudinal functional changes in single RV patients. In a recent study, we were able to show that in patients with HLHS RVEF remains largely unchanged over a period of 10 years after TCPC completions but that indexed RV volumes significantly increase in patients older than 10 years of age.[8]

The present study additionally demonstrates that a decrease in RV strain occurs before a reduction in RVEF becomes apparent. Similar findings were reported by Meyer and colleagues who found a decrease in ventricular strain in Fontan patients with preserved EF over a time period of 2 years using CMR whereas Latus and colleagues did not detect significant changes in CMR-derived myocardial strain and strain rate values.[19,20] However, different to this study, both studies included mixed cohorts of Fontan patients with only a small number of patients with HLHS and the follow-up time was shorter.[19,20] An echocardiographic study from our institution reported a reduction in global strain rate 1.6–5.1 years after TCPC completion in patients with HLHS, but global strain did not change.[6]

Studies in biventricular hearts have shown that GLS of the systemic ventricle is an independent and powerful predictor of outcome,[21,22] not well correlated with EF,[23] and that strain better than EF reflects the systolic function of adult patients with heart disease and preserved EF.[24] The lower sensitivity of EF to the reduction of longitudinal shortening is explained by possibly compensatory GCS predominance, a phenomenon, which was also observed in HLHS studies during staged palliation.[11,25] Ruotsalainen and colleagues demonstrated a significant correlation between vector-velocity-imaging derived strain and strain rate parameters in a horizontal long-axis view and MRI derived EF between the palliation stages but without being a significant predictor of EF.[26] The described independency of GLS is consistent with our findings. Myocardial GLS decreased although RVEF was still largely preserved and a correlation between RVEF and GLS was only observed (Spearman's r=−0.61), when RVEF deteriorated at the time of the third CMR examination. The non-significant GCS changes across the CMR examinations might reflect a shift to circumferential contraction patterns in patients with HLHS.

Although few echocardiographic studies suggest that the size of the left ventricle has no impact on RV function,[27,28] more recent studies point towards the fact that LV size matters.[29–32] Petko and colleagues demonstrated that patients with mitral and aortic atresia with small left ventricles had better septal strain values compared with HLHS subtypes with larger left ventricles using speckle tracking echocardiography.[29] Similar findings were described by 2 other groups by echocardiography[30] and CMR,[31] suggesting that a larger left ventricle particularly impacts septal deformation. Others suggested that apical bulging of the RV is associated with impaired RV strain values and is more commonly found in patients with HLHS with hypertrophied hypoplastic left ventricle.[32] The present study did not investigate the effect on different HLHS subtypes; however, future longitudinal studies should focus on this aspect. Beside geometric properties among HLHS subtypes, treatment strategies,[33] hemodynamically relevant ventricular loading, heart rate,[14,34] and dyssynchrony in contraction caused by activation delay[35] can affect myocardial deformation.

Besides that, RV myocardial mass is in a constant process of change in patients with HLHS due to alternating cardiac conditions during staged palliation and increases significantly during midterm Fontan follow-up. The present findings might be explained by a responsive RV hypertrophy, that creates favorable conditions for ventricular dysfunction by failing to adapt to a more circumferential contraction pattern that would be typical for a left ventricle.[11] Longitudinal shortening accounts for nearly 80% of global RV function in normal hearts[36] and the interventricular septum is responsible for 80% of the RV performance.[37] A relative increase in subepicardial fiber mass after TCPC completion might strengthen circumferential RV free wall shortening to sustain RV performance in patients with HLHS whereas RV longitudinal function declines.

In contrast to the only slight reduction in RVEF the first 2 CMR examinations, myocardial GLS and GLSR decrease significantly during serial follow up in patients with HLHS after Fontan circulation. Thus, caution is advised when assessing RVEF in isolation.

That there is an increase of indexed RV volumes during longitudinal follow in older patients with HLHS

(>10 years) was already recently shown by this group.[8] Potential reasons might be a higher degree of tricuspid regurgitation but also cardiovascular and metabolic changes during puberty with a raise in blood pressure, increased RV afterload and insulin resistance should be taken into account.[38,39]

Certainly, volumetry and analysis of long-axis function using CMR-FT seem to be suitable to detect RV dysfunction. However, further studies are warranted to develop protocols and functional analysis tools best suited to assess the abnormally loaded systemic RV in HLHS.

Factor Analysis

An exploratory factor analysis of 35 parameters between the first and second CMR examination demonstrated high factor loading (>0.5) components revealing the most representative variables which should be considered in particular for RV assessment (Table S2, Figure 4). The results highlight a benefit to combine CMR volumetry and 2D-CMR-FT parameters in patients with HLHS.

Future confirmatory factor analyses in HLHS studies could be supplemented with additional markers to verify and improve the accuracy of the domains found.

Reproducibility Assessment

Interobserver agreement for strain values were lower compared with volumetric parameters, especially for GRS. CMR volumetry is performed from a complete short-axis stack covering the right ventricle from the base to the apex whereas 2D-CMR-FT only uses 3 selected slices from the same stack. Consequently, differences in tracing may have a greater impact on 2D-CMR-FT results and might affect data reproducibility. Nevertheless, intra-observer and inter-observer agreements in 2D-CMR-FT were good for GLS and good to excellent for GCS.

Limitations

This study assessed a large cohort of patients with HLHS in a comparable way but the number of patients with 3 examinations was smaller than those with 2 examinations. Due to the retrospective nature of the study, few CMR data sets were incomplete. In addition, comparisons with echocardiographic measurements were not performed.

The software used for 2D-CMR-FT analysis is designed for hearts with a normal anatomy.[40,41] Myocardial structures are automatically assigned to particular myocardial segments which was more difficult for the

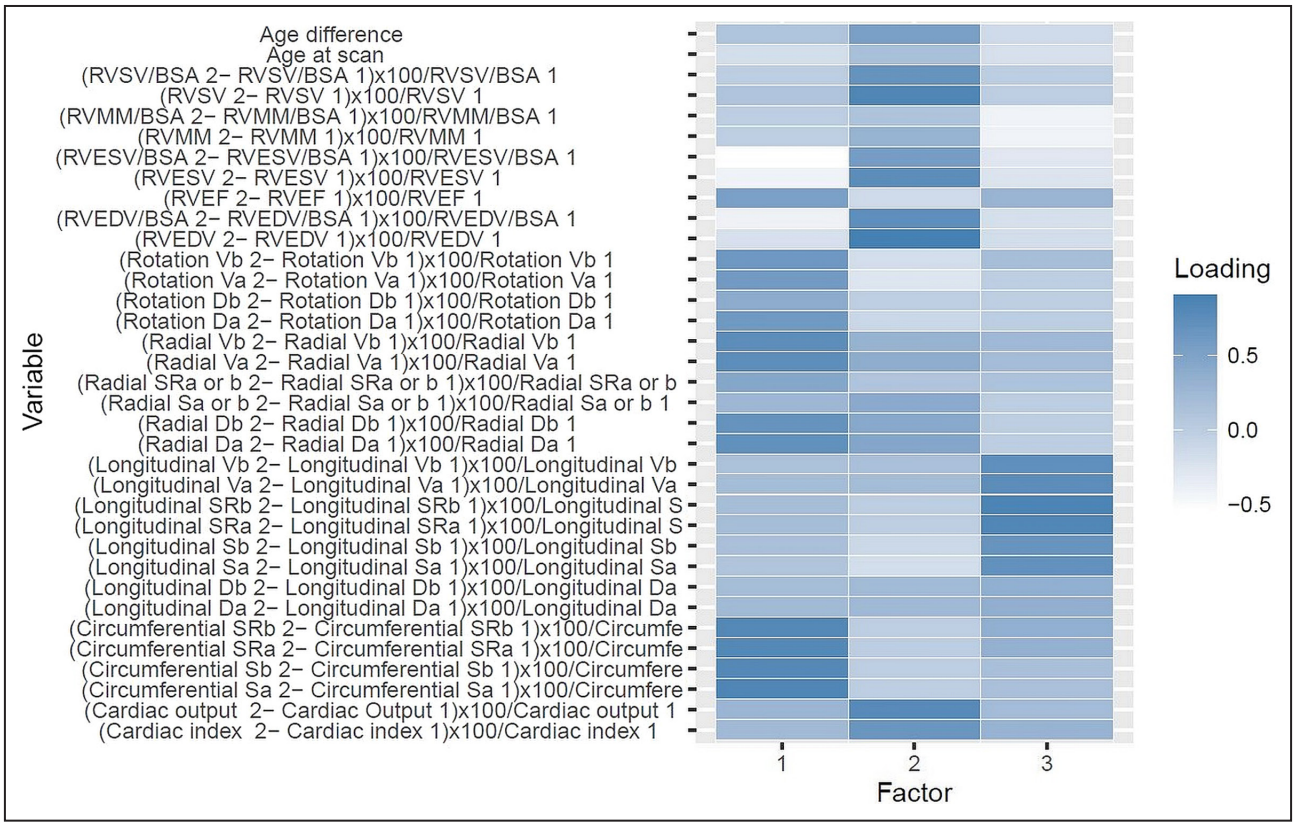

Figure 4. Factor analysis between first and second scan: heatmap of factor loadings, based on relative deviations (variable at second scan−variable at first scan)×100/(variable at first scan).
a, endocardial value; age difference (between CMR scans); b, myocardial value; BSA indicates body surface area; D, displacement; EDV, end-diastolic volume; EF, ejection fraction; ESV, end-systolic volume; i, index; MM, myocardial mass; RV, right ventricle; S, strain; SR, strain rate; SV, stroke volume; and V, velocity.

single right ventricle in patients with HLHS with often coarse trabeculations. Therefore, adaption of manual tracing after automatic segmentation was performed. GLS was assessed from an axial long-axis cine view only, therefore some segments are missing.

General disadvantages of 2D-CMR-FT include a susceptibility to temporal resolution problems and beat-to-beat differences in cine image quality and stability. In addition, accurate tracking of features can fail due to through-plane motion, especially in long-axis views.[42,43]

Furthermore, reduced reproducibility of GRS is a known weakness of 2D-CMR-FT but it does not impact reproducibility of GCS[44] which corresponds to our results.

The influence of comorbidities, medical therapy or sedation on RV measurements were not statistically investigated.

CONCLUSIONS

The results of this study suggest that GLS values decrease earlier than RVEF, indicating that 2D-CMR-FT should routinely be performed in addition to ventricular volumetry to detect early alterations in myocardial deformation and function. Factor analysis might contribute to a rational reduction of data dimension.

ARTICLE INFORMATION

Received January 9, 2022; accepted March 17, 2022.

Affiliations

Department of Congenital Heart Disease and Pediatric Cardiology, University Hospital Schleswig-Holstein, Kiel, Germany (L.M.K., S.B.G., D.D.G., J.H.H., A.S.U., I.V.); Institute of Medical Informatics and Statistics, Kiel University, University Hospital Schleswig-Holstein, Kiel, Germany (S.F.); and DZHK (German Centre for Cardiovascular Research), Partner Site Hamburg/Kiel/Lübeck, Kiel, Germany (D.D.G., J.H.H., A.S.U., I.V.).

Sources of Funding

None.

Disclosures

None.

Supplemental Material

Tables S1–S2

REFERENCES

1. Osiovich H, Phillipos E, Byrne P, Robertson M. Hypoplastic left heart syndrome: "to treat or not to treat". *J Perinatol*. 2000;20:363–365. doi: 10.1038/sj.jp.7200406
2. Tchervenkov CI, Jacobs JP, Weinberg PM, Aiello VD, Béland MJ, Colan SD, Elliott MJ, Franklin RCG, Gaynor JW, Krogmann ON, et al. The nomenclature, definition and classification of hypoplastic left heart syndrome. *Cardiol Young*. 2006;16:339–368. doi: 10.1017/S1047951106000291
3. Voges I, Jerosch-Herold M, Hedderich J, Westphal C, Hart C, Helle M, Scheewe J, Pardun E, Kramer HH, Rickers C. Maladaptive aortic properties in children after palliation of hypoplastic left heart syndrome assessed by cardiovascular magnetic resonance imaging. *Circulation*. 2010;122:1068–1076. doi: 10.1161/CIRCULATIONAHA.109.889733
4. Best KE, Miller N, Draper E, Tucker D, Luyt K, Rankin J. The improved prognosis of hypoplastic left heart: a population-based register study of 343 cases in England and Wales. *Front Pediatr*. 2021;9:635776. doi: 10.3389/fped.2021.635776
5. Siffel C, Riehle-Colarusso T, Oster ME, Correa A. Survival of children with hypoplastic left heart syndrome. *Pediatrics*. 2015;136:e864–e870. doi: 10.1542/peds.2014-1427
6. Michel M, Logoteta J, Entenmann A, Hansen JH, Voges I, Kramer HH, Petko C. Decline of systolic and diastolic 2D strain rate during follow-up of HLHS patients after Fontan palliation. *Pediatr Cardiol*. 2016;37:1250–1257. doi: 10.1007/s00246-016-1424-5
7. Gasparini M, Cox N. Role of cardiac magnetic resonance strain analysis in patients with hypoplastic left heart syndrome in evaluating right ventricular (dys)function: a systematic review. *Eur J Cardiothorac Surg*. 2021;60:497–505. doi: 10.1093/ejcts/ezab105
8. Sobh M, Freitag-Wolf S, Scheewe J, Kanngiesser LM, Uebing AS, Gabbert DD, Voges I. Serial right ventricular assessment in patients with hypoplastic left heart syndrome: a multiparametric cardiovascular magnetic resonance study. *Eur J Cardiothorac Surg*. 2021;61:36–42. doi: 10.1093/ejcts/ezab232
9. Kutty S, Graney BA, Khoo NS, Li L, Polak A, Gribben P, Hammel JM, Smallhorn JF, Danford DA. Serial assessment of right ventricular volume and function in surgically palliated hypoplastic left heart syndrome using real-time transthoracic three-dimensional echocardiography. *J Am Soc Echocardiogr*. 2012;25:682–689. doi: 10.1016/j.echo.2012.02.008
10. Sato T, Calderon RJC, Klas B, Pedrizzetti G, Banerjee A. Simultaneous volumetric and functional assessment of the right ventricle in hypoplastic left heart syndrome after Fontan palliation, utilizing 3-dimensional speckle-tracking echocardiography. *Circ J*. 2020;84:235–244. doi: 10.1253/circj.CJ-19-0926
11. Khoo NS, Smallhorn JF, Kaneko S, Myers K, Kutty S, Tham EB. Novel insights into RV adaptation and function in hypoplastic left heart syndrome between the first 2 stages of surgical palliation. *JACC Cardiovasc Imaging*. 2011;4:128–137. doi: 10.1016/j.jcmg.2010.09.022
12. Salehi Ravesh M, Rickers C, Bannert FJ, Hautemann D, Al Bulushi A, Gabbert DD, Wegner P, Kis E, Hansen JH, Jerosch-Herold M, et al. Longitudinal deformation of the right ventricle in hypoplastic left heart syndrome: a comparative study of 2D-feature tracking magnetic resonance imaging and 2D-speckle tracking echocardiography. *Pediatr Cardiol*. 2018;39:1265–1275. doi: 10.1007/s00246-018-1892-x
13. Schulz-Menger J, Bluemke DA, Bremerich J, Flamm SD, Fogel MA, Friedrich MG, Kim RJ, von Knobelsdorff-Brenkenhoff F, Kramer CM, Pennell DJ, et al. Standardized image interpretation and post-processing in cardiovascular magnetic resonance - 2020 update. *J Cardiovasc Magn Reson*. 2020;22:19. doi: 10.1186/s12968-020-00610-6
14. Ferferieva V, Van den Bergh A, Claus P, Jasaityte R, Veulemans P, Pellens M, La Gerche A, Rademakers F, Herijgers P, D'hooge J. The relative value of strain and strain rate for defining intrinsic myocardial function. *Am J Physiol Heart Circ Physiol*. 2012;302:H188–H195. doi: 10.1152/ajpheart.00429.2011
15. Schlangen J, Petko C, Hansen JH, Michel M, Hart C, Uebing A, Fischer G, Becker K, Kramer HH. Two-dimensional global longitudinal strain rate is a preload independent index of systemic right ventricular contractility in hypoplastic left heart syndrome patients after Fontan operation. *Circ Cardiovasc Imaging*. 2014;7:880–886. doi: 10.1161/CIRCIMAGING.114.002110
16. Motonaga KS, Miyake CY, Punn R, Rosenthal DN, Dubin AM. Insights into dyssynchrony in hypoplastic left heart syndrome. *Heart Rhythm*. 2012;9:2010–2015. doi: 10.1016/j.hrthm.2012.08.031
17. Bharucha T, Khan R, Mertens L, Friedberg MK. Right ventricular mechanical dyssynchrony and asymmetric contraction in hypoplastic heart syndrome are associated with tricuspid regurgitation. *J Am Soc Echocardiogr*. 2013;26:1214–1220. doi: 10.1016/j.echo.2013.06.015
18. Everitt B, Hothorn T. Exploratory factor analysis. In: Gentleman R, Hornik K, Parmigiani P, series eds. *An Introduction to Applied Multivariate Analysis With R*. New York Dordrecht Heidelberg London: Springer Science+Business Media LLC; 2011:135–161.
19. Meyer SL, Ridderbos FS, Wolff D, Eshuis G, van Melle JP, Ebels T, Berger RMF, Willems TP. Serial cardiovascular magnetic resonance feature tracking indicates early worsening of cardiac function in Fontan patients. *Int J Cardiol*. 2020;303:23–29. doi: 10.1016/j.ijcard.2019.12.041
20. Latus H, Kruppa P, Hofmann L, Reich B, Jux C, Apitz C, Schranz D, Voges I, Khalil M, Gummel K. Impact of aortopulmonary collateral flow

and single ventricle morphology on longitudinal hemodynamics in Fontan patients: a serial CMR study. *Int J Cardiol*. 2020;311:28–34. doi: 10.1016/j.ijcard.2020.01.065
21. Kalam K, Otahal P, Marwick TH. Prognostic implications of global LV dysfunction: a systematic review and meta-analysis of global longitudinal strain and ejection fraction. *Heart*. 2014;100:1673–1680. doi: 10.1136/heartjnl-2014-305538
22. Romano S, Judd RM, Kim RJ, Kim HW, Klem I, Heitner JF, Shah DJ, Jue J, White BE, Indorkar R, et al. Feature-tracking global longitudinal strain predicts death in a multicenter population of patients with ischemic and nonischemic dilated cardiomyopathy incremental to ejection fraction and late gadolinium enhancement. *JACC Cardiovasc Imaging*. 2018;11:1419–1429. doi: 10.1016/j.jcmg.2017.10.024
23. Koopman LP, Geerdink LM, Bossers SSM, Duppen N, Kuipers IM, ten Harkel AD, van Iperen G, Weijers G, de Korte C, Helbing WA, et al. Longitudinal myocardial deformation does not predict single ventricle ejection fraction assessed by cardiac magnetic resonance imaging in children with a total cavopulmonary connection. *Pediatr Cardiol*. 2018;39:283–293. doi: 10.1007/s00246-017-1753-z
24. Stokke TM, Hasselberg NE, Smedsrud MK, Sarvari SI, Haugaa KH, Smiseth OA, Edvardsen T, Remme EW. Geometry as a confounder when assessing ventricular systolic function: comparison between ejection fraction and strain. *J Am Coll Cardiol*. 2017;70:942–954. doi: 10.1016/j.jacc.2017.06.046
25. D'Souza R, Wang Y, Calderon-Anyosa RJC, Montero AE, Banerjee MM, Ekhomu O, Matsubara D, Mercer-Rosa L, Agger P, Sato T, et al. Decreased right ventricular longitudinal strain in children with hypoplastic left heart syndrome during staged repair and follow-up: does it have implications in clinically stable patients? *Int J Cardiovasc Imaging*. 2020;36:1667–1677. doi: 10.1007/s10554-020-01870-0
26. Ruotsalainen H, Bellsham-Revell H, Bell A, Pihkala J, Ojala T, Simpson J. Right ventricular systolic function in hypoplastic left heart syndrome: a comparison of velocity vector imaging and magnetic resonance imaging. *Eur Heart J Cardiovasc Imaging*. 2016;17:687–692. doi: 10.1093/ehjci/jev196
27. Schlangen J, Fischer G, Steendijk P, Petko C, Scheewe J, Hart C, Hansen JH, Ahrend F, Rickers C, Kramer H-H, et al. Does left ventricular size impact on intrinsic right ventricular function in hypoplastic left heart syndrome? *Int J Cardiol*. 2013;167:1305–1310. doi: 10.1016/j.ijcard.2012.03.183
28. Wisler J, Khoury PR, Kimball TR. The effect of left ventricular size on right ventricular hemodynamics in pediatric survivors with hypoplastic left heart syndrome. *J Am Soc Echocardiogr*. 2008;21:464–469. doi: 10.1016/j.echo.2007.09.003
29. Petko C, Voges I, Schlangen J, Scheewe J, Kramer HH, Uebing AS. Comparison of right ventricular deformation and dyssynchrony in patients with different subtypes of hypoplastic left heart syndrome after Fontan surgery using two-dimensional speckle tracking. *Cardiol Young*. 2011;21:677–683. doi: 10.1017/S1047951111000631
30. Forsha D, Li L, Joseph N, Kutty S, Friedberg MK. Association of left ventricular size with regional right ventricular mechanics in hypoplastic left heart syndrome. *Int J Cardiol*. 2020;298:66–71. doi: 10.1016/j.ijcard.2019.07.090
31. Wang AP, Kelle AM, Hyun M, Reece CL, Young PM, O'Leary PW, Qureshi MY, Nelson TJ, Haile DT, Miller AR, et al. Negative impact of the left ventricular remnant morphology on systemic right ventricular myocardial deformation in hypoplastic left heart syndrome. *Pediatr Cardiol*. 2021;42:278–288. doi: 10.1007/s00246-020-02480-2
32. Rösner A, Bharucha T, James A, Mertens L, Friedberg MK. Impact of right ventricular geometry and left ventricular hypertrophy on right ventricular mechanics and clinical outcomes in hypoplastic left heart syndrome. *J Am Soc Echocardiogr*. 2019;32:1350–1358. doi: 10.1016/j.echo.2019.06.003
33. Latus H, Nassar MS, Wong J, Hachmann P, Bellsham-Revell H, Hussain T, Apitz C, Salih C, Austin C, Anderson D, et al. Ventricular function and vascular dimensions after Norwood and hybrid palliation of hypoplastic left heart syndrome. *Heart*. 2018;104:244–252. doi: 10.1136/heartjnl-2017-311532
34. Weidemann F, Jamal F, Sutherland GR, Claus P, Kowalski M, Hatle L, De Scheerder I, Bijnens B, Rademakers FE. Myocardial function defined by strain rate and strain during alterations in inotropic states and heart rate. *Am J Physiol - Heart Circ Physiol*. 2002;283:H792–H799. doi: 10.1152/ajpheart.00025.2002
35. Risum N, Jons C, Olsen NT, Fritz-Hansen T, Bruun NE, Hojgaard MV, Valeur N, Kronborg MB, Kisslo J, Sogaard P. Simple regional strain pattern analysis to predict response to cardiac resynchronization therapy: Rationale, initial results, and advantages. *Am Heart J*. 2012;163:697–704. doi: 10.1016/j.ahj.2012.01.025
36. Brown SB, Raina A, Katz D, Szerlip M, Wiegers SE, Forfia PR. Longitudinal shortening accounts for the majority of right ventricular contraction and improves after pulmonary vasodilator therapy in normal subjects and patients with pulmonary arterial hypertension. *Chest*. 2011;140:27–33. doi: 10.1378/chest.10-1136
37. Buckberg G, Hoffman JIE. Right ventricular architecture responsible for mechanical performance: unifying role of ventricular septum. *J Thorac Cardiovasc Surg*. 2014;148:3166–3171.e1-4. doi: 10.1016/j.jtcvs.2014.05.044
38. Van den Eynde J, Danford DA, Doshi A, Kutty S. Right ventricular dysfunction in hypoplastic left heart syndrome: superimposed effects of afterload and insulin resistance in puberty? *Eur J Cardiothorac Surg*. 2022;15:ezac088. doi: 10.1093/ejcts/ezac088
39. Liu Y, Luo Q, Su Z, Xing J, Wu J, Xiang LI, Huang Y, Pan H, Wu X, Zhang X, et al. Suppression of myocardial hypoxia-inducible factor-1α compromises metabolic adaptation and impairs cardiac function in patients with cyanotic congenital heart disease during puberty. *Circulation*. 2021;143:2254–2272. doi: 10.1161/CIRCULATIONAHA.120.051937
40. Maret E, Todt T, Brudin L, Nylander E, Swahn E, Ohlsson JL, Engvall JE. Functional measurements based on feature tracking of cine magnetic resonance images identify left ventricular segments with myocardial scar. *Cardiovasc Ultrasound*. 2009;7:53. doi: 10.1186/1476-7120-7-53
41. Hor KN, Gottliebson WM, Carson C, Wash E, Cnota J, Fleck R, Wansapura J, Klimeczek P, Al-Khalidi HR, Chung ES, et al. Comparison of magnetic resonance feature tracking for strain calculation with harmonic phase imaging analysis. *JACC Cardiovasc Imaging*. 2010;3:144–151. doi: 10.1016/j.jcmg.2009.11.006
42. Obokata M, Nagata Y, Wu VCC, Kado Y, Kurabayashi M, Otsuji Y, Takeuchi M. Direct comparison of cardiacmagnetic resonance feature tracking and 2D/3D echocardiography speckle tracking for evaluation of global left ventricular strain. *Eur Heart J Cardiovasc Imaging*. 2016;17:525–532. doi: 10.1093/ehjci/jev227
43. Bucius P, Erley J, Tanacli R, Zieschang V, Giusca S, Korosoglou G, Steen H, Stehning C, Pieske B, Pieske-Kraigher E, et al. Comparison of feature tracking, fast-SENC, and myocardial tagging for global and segmental left ventricular strain. *ESC Heart Fail*. 2020;7:523–532. doi: 10.1002/ehf2.12576
44. Morton G, Schuster A, Jogiya R, Kutty S, Beerbaum P, Nagel E. Inter-study reproducibility of cardiovascular magnetic resonance myocardial feature tracking. *J Cardiovasc Magn Reson*. 2012;14:43. doi: 10.1186/1532-429X-14-43

SUPPLEMENTAL MATERIAL

Table S1. Additional patient characteristics

Parameters	**1st CMR (n= 108)**	**2nd CMR (n= 108)**	**3rd CMR (n= 41)**
HLHS subtype (n, %)			
- **MA/AA**	46 (42.6%)	46 (42.6%)	19 (46.3%)
- **MS/AS**	30 (27.8%)	30 (27.8%)	11 (26.8%)
- **MS/AA**	26 (24.1%)	26 (24.1%)	9 (22.0%)
- **MA/AS**	6 (5.6%)	6 (5.6%)	2 (4.9%)
Shunt type during Norwood operation (n, %)			
- **BT**	103 (95.4%)	103 (95.4%)	39 (95.1%)
- **Sano**	2 (2.8%)	2 (2.8%)	0 (0%)
- **Central**	3 (1.9%)	3 (1.9%)	2 (4.9%)
Medication (n, %)			
- **Platelet inhibitors**	89 (82.4%)	94 (87.0%)	31 (75.6%)
- **Oral anticoagulant**	13 (12.0%)	14 (13.0%)	8 (19.5%)

- **ACE inhibitors**	46 (42.6%)	23 (21.3%)	12 (29.3%)
- **Beta-blockers**	16 (14.8 %)	9 (8.3 %)	8 (19.5 %)
TR			
- **None (%)**	12 (11.1 %)	5 (4.6%)	1 (2.4%)
- **Trivial (%)**	56 (51.9 %)	44 (40.7 %)	9 (22.0 %)
- **Mild (%)**	31 (28.7 %)	50 (46.3 %)	26 (63.4 %)
- **Moderate (%)**	9 (8.3 %)	9 (8.3 %)	5 (12.2 %)
- **Severe (%)**	0 (0%)	0 (0%)	0 (0%)
Neo-AVR			
- **None (%)**	19 (17.6%)	11 (10.2%)	3 (7.3%)
- **Trivial (%)**	61 (56.5%)	63 (58.3%)	20 (48.8%)
- **Mild (%)**	28 (25.9%)	32 (29.6%)	17 (41.5%)
- **Moderate (%)**	0 (0%)	2 (1.6%)	0 (0%)
- **Severe (%)**	0 (0%)	0 (0%)	1 (2.4%)

ACE, angiotensin converting enzyme; BT, modified Blalock-Taussig shunt; Central, central aortopulmonary shunt; MA/AA, mitral and aortic valve atresia; MS/AS, mitral and aortic valve stenosis; MS/AA, mitral stenosis and aortic valve atresia; MA/AS, mitral atresia

and aortic valve stenosis; Neo-AVR, neo-aortic valve regurgitation; Sano, right ventricle-to-pulmonary artery conduit according to Sano; TR, tricuspid valve regurgitation.

Data are presented as frequencies (%) or median [1st and 3rd quartile].

Table S2. Loadings of the three latent factors between the first and second CMR examination

Parameters	Factor 1	Factor 2	Factor 3
RVEF	0.528		
Rotation Va	0.595		
Rotation Vb	0.624		
Radial Va	0.749		
Radial Vb	0.750		
Rotation Da	0.602		
Radial Da	0.704		
Radial Db	0.685		
Circumferential Sa	0.840		
Circumferential Sb	0.810		
Circumferential SRa	0.811		
Circumferential SRb	0.819		

RVEDV	0.905	
RVESV	0.752	
RVSV	0.838	
RVEDVi	0.738	
RVESVi	0.567	
RVSVi	0.675	
Cardiac output	0.780	
Cardiac index	0.648	
Age difference	0.543	
Longitudinal Va		0.758
Longitudinal Vb		0.737
Longitudinal Sa		0.697
Longitudinal Sb		0.674
Longitudinal SRa		0.834

Longitudinal SRb	0.855

a, endocardial value; age difference (between 1st and 2nd CMR scan); b, myocardial value; D, displacement; EDV, end-diastolic volume; ESV, end-systolic volume; RV, right ventricle; RVEDVi, right ventricular end-diastolic volume index; RVEF, right ventricular ejection fraction; RVESVi, right ventricular end-systolic volume index; RVSVi, right ventricular stroke volume index; S, strain; SR, strain rate; SV, stroke volume; V, velocity.

Factor loadings less than 0.5 are suppressed.